HHS Public Access

Author manuscript

Neuroimage. Author manuscript; available in PMC 2016 May 30.

Published in final edited form as:

Neuroimage. 2016 May 15; 132: 79–92. doi:10.1016/j.neuroimage.2016.02.032.

Unmasking local activity within local field potentials (LFPs) by removing distal electrical signals using independent component analysis

Nathan W. Whitmore and **Shih-Chieh Lin***

Neural Circuits and Cognition Unit, Laboratory of Behavioral Neuroscience, National Institute on Aging, National Institutes of Health, Baltimore, MD 21224, USA

Abstract

Local field potentials (LFPs) are commonly thought to reflect the aggregate dynamics in local neural circuits around recording electrodes. However, we show that when LFPs are recorded in awake behaving animals against a distal reference on the skull as commonly practiced, LFPs are significantly contaminated by non-local and non-neural sources arising from the reference electrode and from movement-related noise. In a data set with simultaneously recorded LFPs and electroencephalograms (EEGs) across multiple brain regions while rats perform an auditory oddball task, we used independent component analysis (ICA) to identify signals arising from electrical reference and from volume-conducted noise based on their distributed spatial pattern across multiple electrodes and distinct power spectral features. These sources of distal electrical signals collectively accounted for 23–77% of total variance in unprocessed LFPs, as well as most of the gamma oscillation responses to the target stimulus in EEGs. Gamma oscillation power was concentrated in volume-conducted noise and was tightly coupled with the onset of licking behavior, suggesting a likely origin of muscle activity associated with body movement or orofacial movement. The removal of distal signal contamination also selectively reduced correlations of LFP/EEG signals between distant brain regions but not within the same region. Finally, the removal of contamination from distal electrical signals preserved an event-related potential (ERP) response to auditory stimuli in the frontal cortex and also increased the coupling between the frontal ERP amplitude and neuronal activity in the basal forebrain, supporting the conclusion that removing distal electrical signals unmasked local activity within LFPs. Together, these results highlight the significant contamination of LFPs by distal electrical signals and caution against the straightforward interpretation of unprocessed LFPs. Our results provide a principled approach to identify and remove such contamination to unmask local LFPs.

Keywords

Movement artifact; Gamma oscillation; Basal forebrain; Event-related potential; $1/f$ power spectrum; Functional connectivity

*Corresponding author at: Neural Circuits and Cognition Unit, Laboratory of Behavioral Neuroscience, National Institute on Aging, National Institutes of Health, 251 Bayview Blvd, Suite 100, 9C220, Baltimore, MD 21224, USA. Tel.: +410 558-8509; fax: +410 558 8328. ; Email: shih-chieh.lin@nih.gov (S.-C. Lin)

The authors declare no competing financial interests.

Introduction

LFPs refer to low-frequency (0–500 Hz) extracellular electrical potentials recorded by microelectrodes within brain tissues, which reflect the aggregate dynamics of synchronized synaptic potentials and population action potentials in local neural circuits (Bédard and Destexhe, 2009; Buzsáki et al., 2012; Destexhe et al., 1999). Recent years have seen surging interest in LFPs, especially in animal models, sparked in part by technological advances that can now record from hundreds of electrodes simultaneously across multiple brain regions (Donoghue, 2002; Nicolelis et al., 1997; Vetter et al., 2004). Recent studies have linked LFPs to the hemodynamic signals underlying fMRI (Logothetis et al., 2001), as well as to magnetoencephalographic (MEG) and EEG signals (Cohen et al., 2009; Nguyen and Lin, 2014; Schroeder et al., 1991; Steinschneider et al., 1992). Recent studies have also shown that LFPs contain information related to cognitive functions and the decision making process with fine spatial and temporal resolution, which was once attributed solely to neuronal spiking activity (Bosman et al., 2012; Hatsopoulos and Donoghue, 2009; Kajikawa and Schroeder, 2011; Katzner et al., 2009; Markowitz et al., 2011; Pesaran et al., 2002). The increasing interest in LFPs recorded in animal models underscores the importance in understanding how LFPs are generated and interpreted.

While LFPs undoubtedly reflect activity in the local circuit surrounding the microelectrode, a largely neglected concern is that LFPs are also affected by electrical signals from distant sources (Kajikawa and Schroeder, 2011). Distal signals can influence LFPs through at least two routes: electrical activity near the reference electrode and volume conduction from distant sources. First, the nature of differential recording entails that LFPs are affected by electrical activity near both the recording electrode as well as the reference electrode (Fein et al., 1988; Lee and Buchsbaum, 1987). While any recording electrode lacking detectable spiking activity can safely serve as the reference site for the purpose of isolating action potentials, the same is not true for recording LFPs because no reference site is devoid of electrical activity (Nunez and Srinivasan, 2006). Second, distant electrical signals can also contribute to LFPs through volume conduction, especially when the distant signal source produces strong electrical fields, such as from movement-related muscle activity (Goncharova et al., 2003; Whitham et al., 2007). A good example of such contamination in the human EEG literature is the eye movement artifact (Gratton et al., 1983; Jung et al., 1998a). The contamination from distant sources may significantly degrade signal-to-noise ratios of LFPs, corrupt power spectral estimates, and inflate coherence between brain regions (Fein et al., 1988). Therefore, the contributions of distant signal sources in LFPs must be recognized and, ideally, identified and removed.

Many methods have been used to attenuate volume-conducted and reference electrode signals in LFPs by leveraging the fact that electrical signals from distant sources should manifest as common activity patterns across many LFP channels. For example, distal electrical signals may be removed during recording by carefully choosing a local reference site for bipolar recording, or analytically removed post-hoc by using methods such as average referencing, current source density analysis, spatial Laplacian transformation (Mitzdorf, 1985; Nunez and Srinivasan, 2006; Nunez et al., 1997; Srinivasan et al., 1998),

or, as we will apply in this study, independent component analysis (ICA) (Bell and Sejnowski, 1995; Jung et al., 1998a; Lee et al., 1999; Makeig et al., 1997).

ICA is a particularly promising technique, which “unmixes” data from an array of electrodes into a set of underlying signal sources, called independent components (ICs), that are temporally independent of each other, with each IC representing a common activity pattern across multiple electrodes (Bell and Sejnowski, 1995; Jung et al., 1998a; Lee et al., 1999; Makeig et al., 1997). ICA has been widely applied in human EEG literature to successfully identify eye movement or electrocardiogram (EKG) artifacts (Jung et al., 1998a, 1998b). ICA has also been applied to LFP recordings in anesthetized animals, for example, from the rat hippocampus, to exclude distant signals sources and to isolate the contributions of distinct input pathways to hippocampal LFPs (Fernandez-Ruiz et al., 2013; Herreras et al., 2015; Korovaichuk et al., 2010; Makarov et al., 2010; Makarova et al., 2014; Martín-Vázquez et al., 2013). The current study extends these previous efforts and applies ICA to analyze LFPs recorded in animals performing behavioral tasks. These are the experimental conditions where LFPs have provided information related to cognitive functions and the decision making process, but also have the greatest potential for contamination from movement-related muscle activity.

The goal of this study is to identify and remove contamination from distal electrical signals in order to unmask local activity within LFPs, and to determine how contaminations from distal signals distorted LFP features. To achieve this goal, we took advantage of a recent data set in which LFPs and EEGs were simultaneously recorded from multiple brain regions while rats performed an auditory oddball task, and applied ICA to identify and remove common activity patterns across multiple channels that were associated with electrical reference activity and volume-conducted noise. We found that, when LFPs were recorded against a distal reference on the skull as commonly practiced, LFP signals were significantly contaminated by non-local and non-neural sources arising from the reference electrode and from movement-related noise. Such contamination systematically distorted LFP responses related to cognitive processes in awake behaving animals. These results caution against the straightforward interpretation of unprocessed LFPs when such contaminations are not accounted for and have broad implications for the proper recording, analysis, and interpretation of LFPs in freely behaving animals.

Materials and methods

All experimental procedures were conducted in accordance with the National Institutes of Health (NIH) Guide for Care and Use of Laboratory Animals and approved by the National Institute on Aging Animal Care and Use Committee. Detailed experimental procedures, regarding behavioral task, surgery, histology, and data collection, have been described in full in a previous report (Nguyen and Lin, 2014). The current paper represents additional analysis of the neurophysiology data collected from that study.

Data sets

The data used in the current study are a subset of 6 recording sessions from 5 male Long–Evans rats performing an auditory oddball task from the data set collected previously in a

separate study (Nguyen and Lin, 2014). These recording sessions were selected because they contain simultaneous recordings of EEGs from the frontal cortex and the primary visual cortex, cortical LFPs from a chronically implanted NeuroNexus linear probe in the frontal cortex, and LFPs and spiking activity from custom-built electrode bundles implanted in the basal forebrain (BF). Electrical signals were amplified using Brighton Omnetics or Cereplex M digital headstages and recorded using a Neural Signal Processor (Blackrock Microsystems, UT). Despite the increasing electrode impedance with decreasing frequencies (Geddes and Roeder, 2001; Nelson et al., 2008), which were measured at 1–25 MΩ at 1 Hz (niPOD, NeuroNexusTech, MI), the high input impedance of these digital headstages (>10 GΩ) was sufficient to prevent significant signal attenuation at frequencies above 1 Hz (Nelson et al., 2008). All sessions contained at least 2 channels of EEG, 29 channels of frontal LFPs, and 5 representative channels of BF LFPs. Data were originally sampled at 2 kHz, then filtered and downsampled to 500 Hz for analysis.

Auditory oddball task

The auditory oddball task (Fig. 1C) contains infrequent-rewarded (oddball, 6 kHz) as well as frequent-unrewarded (standard, 10 kHz) tones, delivered through the same speaker. The stimuli were 0.5 s long and presented at 70 dB SPL. The time between stimulus presentations was 2 s, and the number of standards that were presented in between oddball tones was uniformly drawn from 2, 3, 4, 5, and 6, corresponding to 6–14 s ITI between oddball tones. When the oddball tone was presented, rats could receive reward if they responded within 3 s. Rats were rewarded with 3–5 drops of water reward starting at the 3rd lick of the sipper tube. False alarms during the oddball task reset the ITI timer. Correct behavioral response to the oddball tone (hit) led to reward delivery, as well as a temporary cessation of any tone presentation and the ITI timer until the end of reward consumption.

Recording locations

EEG skull screws were implanted in contact with the dura over the frontal cortex (AP 3.0 mm, ML 3.0 mm relative to bregma) (Paxinos and Watson, 2007) and the primary visual cortex (AP −7.0 mm, ML 4.5 mm) (Fig. 1D). A NeuroNexus linear probe (A1-style, 100 μm spacing, 32-channel, iridium contact sites, 1–3 MΩ impedance measured at 1 kHz) was slowly lowered into the frontal cortex (AP 3.0–4.0 mm, ML −3.0 mm) with the target depth at 4–6.5 mm below cortical surface. A custom-built 32-wire multi-electrode moveable bundle (tungsten, 38 or 16 μm in diameter, with 0.1–0.3 MΩ impedance) was implanted into bilateral BF (AP 0.5 mm, ML ±2.25 mm, DV 7 mm below cortical surface). A common ground screw and a separate reference screw were placed over the right cerebellum (AP −10 mm, 3.0 mm) and left cerebellum (AP −10 mm, −3.0 mm), respectively.

Identification of putative electrical reference and volume-conducted noise using ICA

The method chosen to identify distal electrical signals was based on a blind-source-separation technique known as extended infomax-independent component analysis (ICA), which has been extensively applied to EEG analysis (Jung et al., 1998a; Lee et al., 1999). To facilitate ICA analysis, continuous data from all electrodes were epoched to the onset of the tone. Each epoch encompassed an interval of 500 ms before the trigger to 1000 ms after the

trigger. All data analysis was performed using MATLAB R2013b and EEGLAB 12.0.05b (Delorme and Makeig, 2004) on a 64-bit Intel Mac running OS 10.9.

Data processing proceeded in four steps: artifact rejection, infomax ICA decomposition into independent components (ICs), identification of putative electrical reference signal IC, and identification of putative volume-conducted noise ICs. Putative electrical reference signal and putative volume-conducted noise ICs were subtracted from the uncorrected signals to generate the corrected LFPs/EEGs. These steps are detailed below.

Artifact rejection

Bad channels were first manually identified and excluded from the data set (2 ± 1.8 channels per session; mean ± SD). Bad epochs were rejected based on the joint probability of their kurtosis and amplitude (jointprob function in EEGLAB) with a local threshold of 3 SD and a global threshold of 12 SD (Delorme et al., 2007). On average, 8.5 ± 2.6% (mean ± SD) of epochs were rejected per session. The selected epochs were filtered with an FIR bandpass filter from 0.1 to 100 Hz (−6 db roll-off) in order to improve ICA quality.

Extended infomax ICA

Extended infomax ICA is a blind-source-separation algorithm that decomposes the original signals into an equal number of ICs, while maximizing the independence and non-Gaussianity of each IC (Lee et al., 1999). Because it is a fully blind-source-separation technique, it incorporates no information about the anatomy, electrodes, or characteristics of the reference signal, including their temporal structure. Extended infomax ICA was performed for all data sets using the CUDAICA implementation (Raimondo et al., 2012), which uses NVidia GPUs to accelerate computation. The stopping criteria for ICA were set to a weight change of 1e-9 or a maximum of 3000 steps.

Identification of putative electrical reference

In each session, a reference-like IC was selected among ICs that had a consistent sign (either all positive or all negative) of weighting on all channels (the component did not load positively on some channels and loaded negatively on others). For ICs meeting this criterion, vector angles were calculated between the weights of each IC against the weights of an ideal reference signal (unit vector). Smaller vector angles reflect a highly uniform distribution of weights across channels, similar to the ideal reference.

Two methods were evaluated for their ability to characterize ICs as “reference-like” or “not-reference-like.” In the “minimum-deviance” method, the IC with the smallest vector angle relative to the ideal reference was selected from the set of ICs with consistent sign of weights. For the “clustering method,” a two-mean clustering was applied to all qualified ICs to extract a group of ICs that collectively represented the reference signal. On all measures of performance, differences between the two methods were non-significant, with the exception that the minimum-deviance method showed better consistency across epoch types than the clustering method. Therefore, only the results for the minimum-deviance method are described here.

Identification of putative volume-conducted noise

"Volume-conducted noise" ICs were identified as ICs whose peak frequency in the 10- to 200-Hz range was above 45 Hz. This cutoff was chosen on the basis of a clear bimodal distribution in the peak frequency of ICs (Fig. 2B).

Across 6 sessions, this process yielded a total of 235 ICs (1 IC per channel, ~39.1 good channels per session), of which 6 ICs were classified as electrode reference (1 per session), 182 ICs as local activity, and 47 ICs as volume-conducted noise. We did not exclude any IC in the analysis. By doing so, we mathematically decomposed each LFP/EEG channel into the sum of three sources of signal (Fig. 1A, B).

Power spectra of ICs

The power spectrum in the 1- to 100-Hz range was generated using the *spectopo* function (EEGLAB) for each IC from each data set. To facilitate comparison of power spectra between different ICs, the power spectrum for each IC was normalized by that IC's spectral power in the 5- to 10-Hz range, log-transformed, and then averaged for each type of IC (electrical reference, volume-conducted noise and local activity) (Fig. 2C, D). This normalization was necessary because the absolute power of each IC was not meaningful since the absolute power is scaled by weights in the mixing matrix (Fig. 1B). We chose the 5- to 10-Hz range as the basis for power normalization, which allowed us to compare power spectra across the three types of ICs, and to clearly visualize how the power spectra were aligned with or deviated from the $1/f$ spectrum.

Percent variance accounted for (PVAF)

PVAF was calculated separately for the three types of ICs (electrical reference, volume-conducted noise and local activity) in each LFP and EEG channel. PVAF was then averaged across all LFP channels or EEG channels within each session (Fig. 2E).

Pre/post-correction agreement of event-related potentials (ERPs)

The pre/post-correction agreement of ERPs (Fig. 4A, bottom panel) was calculated using a sliding window cross correlation between ERPs generated by uncorrected and corrected frontal EEG (150 ms window length and 10 ms step). An "N1 window" was defined as the bin spanning 50–200 ms after stimulus onset. Correlation coefficients during the N1 window were compared with those outside of the N1 window using paired *t*-tests.

Event-related spectral perturbation (ERSP)

Prior to estimating ERSPs, EEG signals were subjected to a second round of artifact rejection using pop_jointprob (local and global threshold = 1.5 SD, EEGLAB) since ERSP analysis is more affected by single-trial artifacts than ERP analysis. ERSPs were computed for the oddball hit trials using pop_newtimef function (EEGLAB) with a sliding 0.4 s window and 20 ms step. ERSPs to oddball onset (Fig. 5A) were baseline corrected to spectral power in the −500 to 0 ms period. Long-latency gamma range ERSP was defined as the change in spectral power at 40–100 Hz during the 300- to 1000-ms window after stimulus onset. To further determine the origin of the gamma oscillation power increase,

EEG signals were re-aligned to the first lick response for lick clusters beginning within the response window to an odd tone (hits) and lick clusters beginning outside the response window (false alarms) (Fig. 5C, D). Power in the gamma range was calculated by first filtering signals with an FIR bandpass filter from 40 to 100 Hz (- 6 db roll-off), followed by the Hilbert transform of the filtered data with a 48-ms-wide Hanning window smoothing of its amplitude.

Correlations of LFPs and EEGs within and between brain regions

For each session, correlation coefficients were computed between each pair of LFP channels. *R* values were then pooled across all sessions by electrode location to generate between and within area estimates (Fig. 6). LFPs and EEGs from the frontal cortex were treated as signals from two different brain regions.

Functional coupling between BF bursting activity and frontal LFPs

BF bursting neurons were identified as previously described (Nguyen and Lin, 2014). The spiking activity of all BF bursting neurons in the same session was pooled together, binned at 1 ms and epoched in the [− 0.5,1] s window corresponding to the LFP epochs. The amplitudes of the evoked responses to tone were calculated in each trial (including both oddball and standard trials) for each of the frontal LFPs (baseline-corrected mean voltage in the 50- to 200-ms window) and for the pooled BF bursting neuron activity (mean firing rate in the 50- to 200-ms window). The functional coupling between each frontal LFP channel and BF bursting activity was defined as the absolute correlation coefficient between the amplitude of the frontal LFP and the BF bursting amplitude across trials.

Reliability across ICA runs

To calculate the reliability of ICA in identifying the same distal electrical signals, each session was submitted to three different ICA decomposition runs. Reliability was measured by computing the correlation coefficient between the pooled distal electrical signals (including both electrical reference and volume-conducted noise) in each channel across compositions.

Results

We hypothesized that the recorded LFP signals consist of at least three distinct types of signal sources: local electrical activity near the microelectrode, electrical activity near the reference electrode, and other volume-conducted noise from sources outside of the brain (Fig. 1A). The latter two types of signals arise from distant sources and degrade the signal-to-noise ratio of true local activity in LFPs. We sought to identify these two types of distant signals based on the idea that strong distant signal sources can influence many channels across multiple brain regions simultaneously, and will thus generate common patterns of activity fluctuations. This is not the case for local electrical activity near the microelectrode, which quickly decays over space (Destexhe et al., 1999; Katzner et al., 2009; Kajikawa and Schroeder, 2011). Common activity patterns spanning multiple recording electrodes therefore may provide the signature of distant signal sources.

In order to identify distant signal sources based on common activity patterns across electrodes and brain regions, we applied a blind-source-separation method: independent component analysis (ICA) (Bell and Sejnowski, 1995; Lee et al., 1999) (Fig. 1B). ICA has been used in EEG analysis to successfully identify and remove distant signal sources such as eye movement and EKG artifact (Jung et al., 1998a, 1998b) as well as in the analysis of LFP signals in anesthetized animals to remove distant signal sources (Korovaichuk et al., 2010; Makarova et al., 2014). The successful identification of underlying sources using ICA requires simultaneous recording of multiple LFPs across multiple brain regions. We therefore took advantage of a recent data set in which multiple LFPs and EEGs were recorded while rats performed an auditory oddball task, in which the occasional presentation of the oddball sound signaled the availability of reward (Fig. 1C, $n = 5$ rats, 6 sessions) (Nguyen and Lin, 2014). Multiple LFPs were simultaneously recorded in the basal forebrain (BF) and across all layers of the frontal cortex, along with EEG recordings in the frontal and the visual cortex. All signals were referenced against a distant skull screw over the cerebellum (Fig. 1D). This data set allowed us to establish that a prominent N1-like event-related potential (ERP) in the frontal cortex is tightly coupled with, and likely generated by, phasic bursting activity of non-cholinergic BF neurons (Nguyen and Lin, 2014; Raver and Lin, 2015).

Applying ICA to this data set served to “unmix” LFPs/EEGs into underlying signal sources called independent components (ICs) and a corresponding mixing matrix, which specifies the weights in which ICs can be combined to reconstruct the original signals (Fig. 1B). Each underlying signal source can be characterized by the power spectral content of each IC and its spatial distribution across different electrodes. Based on the ICA transformation, we sought to identify the ICs associated with electrical reference and with volume-conducted noise, such that the removal of those ICs would lead to “corrected” LFPs that better represent local activity near recording electrodes.

We first sought to identify the ICs associated with electrical reference. In differential recording configurations, the electrical activity near the reference electrode is subtracted from electrical activity recorded from all electrodes. Therefore, the electrical reference signal should be reflected in all recording channels with near-identical weights. To identify the IC associated with electrical reference, all ICs within the same session were classified into two groups based on whether their weights on all channels share the same sign. In the group of ICs with a consistent sign of weights across channels, we designated the IC with the least amount of weight fluctuation across channels as the putative electrical reference signal (Fig. 2A), which represents a common distal signal source that has near-identical influences on all channels. As expected, electrical reference ICs exhibited much less variation in weight across channels than the other two signal sources (Fig. 2A).

Next, we sought to identify ICs associated with volume-conducted noise among the remaining ICs. We noted that a subset of ICs had a distinct peak of spectral power at frequencies ≥45 Hz ($n = 47$, average 7.8 ICs per session, Fig. 2B). The bimodal distribution of ICs suggests that these two types of ICs may correspond to two distinct signal sources. As we discuss in subsequent analyses, ICs with aberrant peak frequencies ($n = 47$) have

properties that correspond to volume-conducted noise arising from distal sources, while the remaining ICs (n = 182) likely correspond to true local activity.

While the spectral information was not used in the ICA analysis, putative local activity ICs showed the typical $1/f$ power-frequency relationship commonly observed in LFPs (Fig. 2C, D) (Bédard et al., 2006; Novikov et al., 1997). The $1/f$ characteristic, however, was not observed in electrical reference signals (Fig. 2C) or in volume-conducted noise (Fig. 2D). The volume-conducted noise ICs had spectral peaks that were either narrow and associated with power line noise at 60 Hz, or broader peaks (40–60 Hz) that likely corresponded to the frequency band of aggregate muscle EMG activity (Goncharova et al., 2003; Whitham et al., 2007), suggesting that volume-conducted noise likely arises from signal sources outside the brain. The power spectra of electrical reference signal also deviated from the $1/f$ power-frequency scaling, especially at higher frequencies. In some cases, the reference IC contained distinct peaks at frequencies greater than 45 Hz similar to volume-conducted noise ICs, suggesting that line noise or EMG activity may also contribute to the identified electrical reference. These results show that while the ICA algorithm is blind to the power spectral content of the underlying signal sources, ICA was able to unmix the original LFP/EEG signals into putative local activities that follow the $1/f$ power-frequency relationship and distal signal sources that deviate from the $1/f$ relationship. Additional analyses linking volume-conducted noise to muscle activity associated with onset of movement will be discussed in Fig. 5.

An example of how the recorded signals were partitioned into three distinct signal sources is shown in Fig. 3A. This example illustrates how common fluctuations across channels were captured by distal electrical signals and removed from the reconstructed local activity. Across sessions, there was a large variability in the respective contributions of the three signal sources (Fig. 2E). Distal electrical signals, in aggregate, accounted for between 8% and 89% of the total variance in EEGs, and between 23% and 77% of the variance in LFPs. The high percentage of total variance accounted for by distal electrical signals suggests that their removal will significantly enhance the signal-to-noise ratio of true local activity in EEGs and LFPs.

To verify that the removal of distal electrical signals left intact the true local activity within EEGs and LFPs, we tested whether the reconstructed local activity in LFPs captured most of the event-related potential (ERP) responses in EEGs and LFPs. This is to be expected if ERPs reflected local LFP activity and were not generated by distal electrical signals. As shown in the example session in Fig. 3B and for all sessions in Fig. 4, the ERP responses in frontal EEG and LFPs were largely preserved by the reconstructed local activity, while the electrical reference and volume-conducted noise contributed little to the averaged response. In the original study using the auditory oddball task (Nguyen and Lin, 2014), Nguyen and Lin found that the oddball stimulus elicited a prominent N1-like ERP response in the frontal EEG and associated positive LFP responses in the deep layers of the underlying frontal cortical circuits. In the current study, we found that the similarity between corrected and uncorrected frontal ERPs was highest during the N1-like ERP window compared with windows before or after (Fig. 4A). This indicates that the prominent N1-like ERP response was faithfully preserved by the corrected local activity in the frontal EEG. Likewise, the

layer-specific distribution of LFP responses associated with the N1-like ERP was also preserved in the corrected local activity of frontal LFPs (Fig. 4B). Moreover, the removal of distal electrical signals in the frontal EEG reduced the between-subject variability of longer latency ERPs subsequent to the N1-like ERP component and produced a similar P3-like ERP response in most sessions (Fig. 4A). The removal of distal electrical signals also made the layer-specific distribution of LFP responses more similar between the two sessions from the same animal (sessions 1 and 5 in Fig. 4B). These results indicate that while the reconstructed local activities in LFPs and EEGs only represent a fraction of total variance of the uncorrected data, they faithfully capture most of the event-related responses and likely resemble true local activity.

While the removal of distal electrical signals had little influence on the N1-like ERP component, we found that the removal of distal electrical signals had a significant impact on the event-related spectral perturbation (ERSP) at longer latencies. In both frontal and visual cortex EEGs, the prominent increases in gamma oscillation power (40–100 Hz) after 300 ms of oddball stimulus onset were significantly reduced after the removal of distal electrical signals (Fig. 5A, B, $p = 0.021$, paired t-test). The increased gamma power was instead largely preserved in the volume-conducted noise (Fig. 5A, B). Furthermore, in contrast to the highly similar pattern of gamma power increase in volume-conducted noise in both EEG channels (Fig. 5A, bottom panels), the removal of distal electrical signals had little impact at lower frequencies on the initial power increase coincident with the N1-like ERP in the frontal cortex, as well as the subsequent long-lasting power decreases in the visual cortex (Fig. 5A, middle panels). High-frequency, long-latency activity was also reduced to approximately the same extent in the frontal-V1 bipolar derivation, an established technique for eliminating spurious gamma oscillations in humans (Nagasawa et al., 2011). These observations support that the increased gamma oscillation power in EEGs was not generated locally around recording electrodes but originated from common distal sources.

While the gamma power increase in volume-conducted noise was loosely time-locked to stimulus onset, it was tightly coupled with the initiation of licking response (Fig. 5C, D). The coupling between gamma oscillation power and the initiation of licking behavior was qualitatively similar in both rewarded (hits) and unrewarded licking responses (false alarms) and largely absent within corrected local activity (Fig. 5C, D). The increase in gamma power in volume-conducted noise also shares many common features with EMG activity (Goncharova et al., 2003; Whitham et al., 2007): peak frequencies, long durations, weakly phase-locked to stimulus onset, present on multiple electrodes, and time-locked to the onset of licking movement. These similarities suggest that EEG gamma power increases following oddball stimulus onset are largely contributed by EMG activity outside of the brain.

We further predict that the removal of distal electrical signals should significantly reduce the functional coupling between LFP and EEG signals. To test this prediction, we quantified the cross correlation for all pairs of un-averaged LFPs and EEGs within the same brain region or between brain regions (Fig. 6). In the uncorrected data, we observed strong correlations between pairs of LFPs/EEGs in all combinations. Removing distal electrical signals significantly reduced correlations in all combinations between distant brain regions and completely abolished the correlation in one case (visual cortex EEG vs. BF LFPs).

Correlations of LFPs within the same brain region were either not affected or were slightly enhanced after removing distal electrical signals. On the other hand, the aggregate volume-conducted noise was highly correlated across distant brain regions compared to local activity, and therefore represents a widely distributed signal source and unlikely to represent local activity within a brain region. We also noted that volume-conducted noise appeared to be less correlated between LFPs recorded within the same region (frontal cortex or BF) compared to local activity. We speculate that the reason behind this reversal was that these LFP recording sites were closer to the putative signal source (i.e., licking-related muscles), and therefore the electric fields may be more complex and heterogeneous. Together, these results support our prediction that distal electrical signals significantly inflated the functional coupling between distant brain regions.

While the properties of reconstructed LFPs discussed thus far resembled true local activities near the recording microelectrodes, the removal of common signals across channels necessarily predicted, at least qualitatively, the distortion of power spectra (Fig. 5) and reduction of coupling between LFPs/EEGs (Fig. 6). Further validation of the claim that removing distal electrical signals improved the signal-to-noise ratio of local LFPs would require an independent measure not processed by ICA, such as spiking activity. One scenario offering such a test is the coupling between N1-like frontal ERP and the phasic bursting activity of non-cholinergic BF neurons (Nguyen and Lin, 2014). We reasoned that, if reconstructed LFPs had higher signal-to-noise ratios and more closely approximated local activity, the reconstructed LFPs should show stronger coupling with BF bursting activity compared with uncorrected LFPs. An example of such coupling is illustrated in Fig. 7A, where a frontal LFP channel was noisy and only weakly coupled with BF bursting activity before correction but showed significantly stronger coupling with BF bursting strength in single trials after the removal of distal electrical signals. Overall, corrected frontal LFPs indeed showed stronger correlations with BF bursting activity (Fig. 6B). Moreover, the increase in the BF-frontal LFP correlation was negatively correlated with the percentage of total variance in LFPs explained by local activity (Fig. 6C) and hence positively correlated with the percentage of total variance explained by distal electrical signals. These results support the conclusion that reconstructed LFPs better resemble local activity near the recording electrodes compared to uncorrected LFPs. They also strengthen the observation that the N1-like frontal ERP is coupled with BF bursting activity in single trials (Nguyen and Lin, 2014).

Finally, we investigated whether ICA can reliably identify the same electrical reference signal and volume-conducted noise from the same data set. Each session of data was subjected to three separate runs of ICA decomposition to reconstruct aggregate distal electrical signals that included both electrical reference signal and volume-conducted noise. The correlation coefficient of the pooled volume-conducted noise and electrical reference between different runs was 0.98 ± 0.002 (mean ± SEM, range = 0.62–1). Thus, distal electrical signals can be reliably identified in most cases.

Discussion

Here we proposed and validated a method to unmask local activity within LFPs by identifying and removing distal electrical signals using independent component analysis (ICA) (Figs. 1 and 3). Distal electrical signals from electrical reference and volume-conducted noise from outside the brain significantly degraded LFP signals and collectively accounted for 23–77% of LFP variance (Fig. 2). The reconstructed LFPs better approximated local activity around microelectrodes because they displayed characteristic $1/f$ power spectra (Fig. 2), preserved the N1-like ERP response and its layer-profile to the oddball stimulus (Fig. 4), and increased the correlation with basal forebrain bursting activity (Fig. 7). The removal of distal electrical signals, however, significantly reduced gamma power increases to the oddball stimulus in EEGs (Fig. 5) and reduced coupling of LFPs/EEGs between brain regions (Fig. 6). These results show that true local activity only accounts for a small portion of total variance in LFPs recorded against a distal skull screw reference in awake behaving rats. Given the increasing interest in LFPs and their wide applications, our results have broad implications for how to properly record, analyze, interpret, and report LFP activity, especially in awake behaving animals.

Validation of ICA in identifying distal electrical signals

Several observations support the idea that the bimodal distribution of ICs (Fig. 2B) correspond to two distinct signal sources, one representing local activity while the other representing volume-conducted noise. First, while spectral information was not used in the ICA analysis, ICA was able to unmix EEGs and LFPs into two types of ICs that have distinct power spectra: one with $1/f$ spectra and the other significantly deviated from $1/f$ spectra with peak frequency in 45–60 Hz (Fig. 2D). The $1/f$ power-frequency relationship has been established as a key property of LFPs (Bédard and Destexhe, 2009). Second, compared to the $1/f$ spectra, the putative volume-conducted noise showed elevated power with spectral peaks in the range of 30–80 Hz, which have been associated with EMG contamination (Goncharova et al., 2003; Whitham et al., 2007) and with line noise artifact. Third, the gamma range oscillation in the putative volume-conducted noise components—but not in putative local components—was associated with licking behavior that involves movement of the body and orofacial muscles (Fig. 5C, D). A transient increase in gamma oscillation power was tightly coupled with the start of licking behavior, regardless of whether such licking response was rewarded or not. Such a pattern suggests that the increase in gamma was not coupled with cue onset nor the receipt of reward, and most likely originated from muscle activity associated with body movement or orofacial movement. Fourth, the aggregate volume-conducted noise was highly correlated across brain regions compared to local activity ICs (Fig. 6) and therefore represents a widely distributed signal source and unlikely to represent local activity within a brain region.

We noted that the spectra of electrical reference signals also deviated from $1/f$ relationship and, in some cases, displayed spectral peaks similar to the volume-conducted noise (Fig. 2C, D). This observation suggests that the reference electrode—a skull screw over the cerebellum in our studies—is similarly susceptible to volume-conducted noise outside of the

brain and can indirectly relay such noise to recorded LFP activity in the common reference configuration.

The putative electrical reference that we identified represents a global signal that has near-identical influences on all electrodes. While we suggest that the source of this global signal is likely the electrical activity from the common reference electrode, this global signal may also originate from other strong neural signals outside of the recording region(s) that generate near-identical signals on all electrodes through volume conduction. Regardless of its origin, the observation that the global signal has consistent influences across widely separated electrodes in different anatomical regions implies that the global signal represents a signal source distal to all LFPs and EEGs and should be analytically removed.

While the removal of selected ICs necessarily predicts a reduction in cross-channel coupling as well as changes in power spectral responses, the consistent response patterns in corrected LFPs suggest that corrected LFPs better approximated true local signals around microelectrodes. Furthermore, this conclusion is independently supported by the enhanced correlation with spiking activity in the BF (Fig. 7), which was not processed by ICA. BF bursting activity is known to evoke an ERP response in the frontal cortex both when BF is electrically stimulated, and when an oddball stimulus is presented (Nguyen and Lin, 2014). Our observation that removing distal electrical signals increased the trial-by-trial correlation between BF bursting strength and frontal LFP amplitude (Fig. 7) therefore reflects an increase in the signal-to-noise ratio of true local activity in corrected LFPs.

The source of gamma oscillations

As discussed in the last section, several observations led us to suggest that gamma oscillations in volume-conducted noise likely originated from extracranial muscle activity. These observations include the similarity of power spectra with peaks in the gamma range (Fig. 2D), tight coupling with licking behavior (Fig. 5C, D), and the widespread spatial distribution across distant brain regions (Fig. 6). In addition, gamma oscillation responses in EEGs were greatly reduced in the frontal-V1 bipolar EEG derivation (Fig. 5A, B), which further supports the idea that long-latency gamma responses in our data set, at least in the EEGs, was generated from a distal source and not local to either frontal cortex or V1. We also note that while the volume-conducted noise only accounted for less than 10% of variance in EEGs (Fig. 2E), they accounted for the vast majority of EEG gamma responses.

The gamma oscillations in volume-conduced noise are also very different from the local sources of gamma oscillation commonly described in human ECoG studies, which typically peak at higher frequencies (60– 200 Hz) and are very spatially localized and task-specific (Crone et al., 2006; Kojima et al., 2013). By contrast, the volume-conducted noise that we seek to remove has a wide spatial distribution and has lower frequencies (40–60 Hz), consistent with studies of EMG contamination in humans (Goncharova et al., 2003; Whitham et al., 2007). In fact, gamma oscillations attributed to volume-conducted noise that our current study seeks to identify and analytically remove is the same type of noise human ECoG recordings seek to minimize through preprocessing measures, including reformatting ECoG signals to a common average reference to reduce the influence from common distal

signal sources (Crone et al., 2006), as well as using EOG and EMG activity to exclude epochs with muscle artifact (Kojima et al., 2013).

While our original study did not record EMG activity from orofacial muscles, previous studies have shown that licking in rodents and rabbits is associated with a highly stereotypical pattern of activity involving muscles of the jaw and the tongue, including temporalis, masseter, digastric muscles, and others (Yamamoto et al., 1982; Liu et al., 1998; Kobayashi et al., 2002; Uchida et al., 1994) The tightly coordinated activity of multiple licking-related muscles likely can generate strong dipoles capable of affecting the signals detected at distant electrodes inside the brain. Given that even small movements in humans, such as microsaccades, can generate significant gamma range electrical artifact (Yuval-Greenberg et al., 2008), it is conceivable that the activation of powerful orofacial muscles in rodents can similarly generate electrical artifacts in EEGs and LFPs in the gamma oscillation range. However, exactly how activities of individual muscles are propagated, filtered and combined together to generate gamma range artifact in EEGs and LFPs is beyond the scope of the current study.

Comparison with other methods to remove distal electrical signals

A key factor that allowed us to identify and remove distal electrical signals is the simultaneous recording of many LFP signals across multiple brain regions. The dense sampling of local variability in LFPs within the same brain region makes it possible to analytically distinguish local activity from distal electrical signals present across multiple electrodes using ICA.

Our method of removing distal signals based on their common activity patterns over multiple electrodes is conceptually similar to approaches in human EEG studies such as bipolar recording, average reference, scalp Laplacian transform, and current source density (CSD) estimates in LFP studies (Mitzdorf, 1985; Nunez and Srinivasan, 2006; Nunez et al., 1997; Srinivasan et al., 1998). These methods rely ondifferences between pairs or groups of local electrodes to impose a spatial high pass filter on the data, and therefore reduce the contribution of far-field influences from distal signals such as electrical reference and muscle artifacts. However, these methods have assumptions about the underlying topography of electric fields and often require electrodes to be placed in a particular spatial pattern (Mitzdorf, 1985; Nunez and Westdorp, 1994; Zaveri et al., 2006). For example, while local referencing strategies such as bipolar recording has the advantage of effectively eliminating volume conduction signals arising outside the region of interest, bipolar montages can also attenuate the amplitude of local activity in LFPs in an unpredictable manner that depends on the spatial distribution of local LFPs and the precise locations of both electrodes in the bipolar pair. It has also been suggested that CSD analysis based on LFPs may not be ideal because removing DC-coupled signals during LFP recording may result in different amounts of baseline offset in individual LFP channels, leading to spurious estimation of sources and sinks in CSD analysis (Herreras et al., 2015; Martín-Vázquez et al., 2013).

Unlike other methods discussed above, the ICA-based method is minimally dependent on the precise location of the electrodes (Makarova et al., 2014). Using ICA to remove electrical reference can be viewed as re-referencing LFPs to a new reference site at a virtual

location, which has no local activity, thereby minimizing the contribution of LFPs from the reference site. Similar methods have been developed in the human EEG literature to identify and remove electrical reference using blind source separation (Hu et al., 2007; Ranta et al., 2010), as well as in the analysis of LFP signals in anesthetized animals to remove distant signal sources (Korovaichuk et al., 2010; Makarova et al., 2014).

The current study extends these previous efforts and applies ICA to analyze LFPs recorded while animals perform behavioral tasks. These are the experimental conditions where LFPs and EEGs have been linked to cognitive functions but are also most susceptible to contamination from movement-related muscle activity. Indeed, our results highlight the significant contributions of movement-related muscle activity to EEGs and LFPs in such conditions, which can degrade LFP quality directly through volume conduction, or indirectly through affecting the electrode reference. Our results show that ICA provides a principled approach to reconstruct local LFP activity.

Implications for LFP studies in freely moving animals

The current study was inspired by the common use of ICA in human EEG studies to remove electrical artifacts from extracranial sources such as eye movement. While it is widely recognized in human EEG and ECoG studies that extracranial muscle activity can lead to widespread electrical artifact, it is not a well-recognized issue in animal studies especially with regard to LFPs. Our results suggest that the contamination of LFPs by muscle artifact is a serious but under-appreciated issue in animal studies, especially in freely moving animals when their movements are not constrained.

The results from the current study caution against the straightforward interpretation of unprocessed LFPs and EEGs in awake behaving animals—including ERPs, ERSPs, and functional connectivity analysis— when the contaminations from distant signal sources are not accounted for. Contaminations from distal electrical signals degrade signal-to-noise ratio of true local LFPs (Figs. 2 and 3). They also bias power spectral estimates (Fig. 5) and inflate coherence and correlation estimates between distal brain regions (Fig. 6). Moreover, the increase in gamma oscillation power in EEGs was largely accounted for by the presence of gamma power in distal electrical signals (Fig. 5), which likely reflects muscle activity contamination and does not reflect local cortical activity. While such a finding does not imply that local gamma synchronization does not occur in the cortex, these results urge caution in ascribing cognitive significance to gamma-band responses in freely moving animals before ruling out the contribution of volume-conducted muscle activity (Goncharova et al., 2003; Keren et al., 2010; Whitham et al., 2007). Finally, given that the contamination from distal electrical signals is tightly coupled with onset of licking behavior, such signals likely originate from stereotypical orofacial movements associated with the onset of licking and may similarly degrade LFP signals recorded in head-restrained animals.

Acknowledgments

This research is funded by the intramural research program of the National Institute on Aging, NIH and by a NARSAD Young Investigator Award to SL. We thank D.P. Nguyen for collecting the original data set; H.M.V. Manzur, S.M. Raver, and P.R. Rapp for critical discussions and reading of the manuscript; H.M.V. Manzur and B. Brock for technical help.

References

Bédard C, Destexhe A. Macroscopic models of local field potentials and the apparent 1/f noise in brain activity. Biophys. J. 2009; 96:2589–2603. [PubMed: 19348744]

Bédard C, Kröger H, Destexhe A. Does the 1/f frequency scaling of brain signals reflect self-organized critical states? Phys. Rev. Lett. 2006; 97:118102. [PubMed: 17025932]

Bell AJ, Sejnowski TJ. An information-maximization approach to blind separation and blind deconvolution. Neural Comput. 1995; 7:1129–1159. [PubMed: 7584893]

Bosman CA, Schoffelen JM, Brunet N, Oostenveld R, Bastos AM, Womelsdorf T, Rubehn B, Stieglitz T, De Weerd P, Fries P. Attentional stimulus selection through selective synchronization between monkey visual areas. Neuron. 2012; 75:875–888. [PubMed: 22958827]

Buzsáki G, Anastassiou CA, Koch C. The origin of extracellular fields and currents—EEG, ECoG, LFP and spikes. Nat. Rev. Neurosci. 2012; 13:407–420. [PubMed: 22595786]

Cohen J, Heitz R, Schall J, Woodman G. On the origin of event-related potentials indexing covert attentional selection during visual search. J. Neurophysiol. 2009:2375–2386. [PubMed: 19675287]

Crone NE, Sinai A, Korzeniewska A. High-frequency gamma oscillations and human brain mapping with electrocorticography. Prog. Brain Res. 2006; 159:275–295. [PubMed: 17071238]

Delorme A, Makeig S. EEGLAB: An open source toolbox for analysis of single-trial EEG dynamics including independent component analysis. J. Neurosci. Methods. 2004; 134:9–21. [PubMed: 15102499]

Delorme A, Sejnowski T, Makeig S. Enhanced detection of artifacts in EEG data using higher-order statistics and independent component analysis. NeuroImage. 2007; 34:1443–1449. [PubMed: 17188898]

Destexhe A, Contreras D, Steriade M. Spatiotemporal analysis of local field potentials and unit discharges in cat cerebral cortex during natural wake and sleep states. J. Neurosci. 1999; 19:4595–4608. [PubMed: 10341257]

Donoghue JP. Connecting cortex to machines: recent advances in brain interfaces. Nat. Neurosci. 2002; 5(Suppl):1085–1088. [PubMed: 12403992]

Fein G, Raz J, Brown FF, Merrin EL. Common reference coherence data are confounded by power and phase effects. Electroencephalogr. Clin. Neurophysiol. 1988; 69:581–584. [PubMed: 2453336]

Fernandez-Ruiz A, Munoz S, Sancho M, Makarova J, Makarov VA, Herreras O, Ferna A, Mun S, Sancho M, Makarova J, et al. Cytoarchitectonic and dynamic origins of giant positive local field potentials in the dentate gyrus. J. Neurosci. 2013; 33:15518–15532. [PubMed: 24068819]

Geddes LA, Roeder R. Measurement of the direct-current (faradic) resistance of the electrode-electrolyte interface for commonly used electrode materials. Ann. Biomed. Eng. 2001; 29:181–186. [PubMed: 11284673]

Goncharova II, McFarland DJ, Vaughan TM, Wolpaw JR. EMG contamination of EEG: spectral and topographical characteristics. Clin. Neurophysiol. 2003; 114:1580–1593. [PubMed: 12948787]

Gratton G, Coles MG, Donchin E. A new method for off-line removal of ocular artifact. Electroencephalogr. Clin. Neurophysiol. 1983; 55:468–484.

Hatsopoulos NG, Donoghue JP. The science of neural interface systems. Annu. Rev. Neurosci. 2009; 32:249–266. [PubMed: 19400719]

Herreras O, Makarova J, Makarov VA. New uses of LFPs: pathway-specific threads obtained through spatial discrimination. Neuroscience. 2015

Hu S, Stead M, Worrell GA. Automatic identification and removal of scalp reference signal for intracranial EEGs based on independent component analysis. IEEE Trans. Biomed. Eng. 2007; 54:1560–1572. [PubMed: 17867348]

Jung T-P, Humphries C, Lee T-W, Makeig S, McKeown MJ, Iragui V, Sejnowski TJ. Extended ICA removes artifacts from electroencephalographic recordings. Adv. Neural Inf. Process. Syst. 1998a; 10:894–900.

Jung, T-P.; Humphries, C.; Lee, T-W.; Makeig, S.; McKeown, MJ.; Iragui, V.; Sejnowski, TJ. Removing electroencephalographic artifacts: comparison between ICA and PCA. Neural Networks

for Signal Processing VIII, 1998; Proceedings of the 1998 IEEE Signal Processing Society Workshop; 1998b. p. 63-72.

Kajikawa Y, Schroeder CE. How local is the local field potential? Neuron. 2011; 72:847–858. [PubMed: 22153379]

Katzner S, Nauhaus I, Benucci A, Bonin V, Ringach DL, Carandini M. Local origin of field potentials in visual cortex. Neuron. 2009; 61:35–41. [PubMed: 19146811]

Keren AS, Yuval-Greenberg S, Deouell LY. Saccadic spike potentials in gamma-band EEG: characterization, detection and suppression. NeuroImage. 2010; 49:2248–2263. [PubMed: 19874901]

Kobayashi M, Masuda Y, Fujimoto Y, Matsuya T, Yamamura K, Yamada Y, Maeda N, Morimoto T. Electrophysiological analysis of rhythmic jaw movements in the freely moving mouse. Physiol. Behav. 2002; 75:377–385. [PubMed: 11897265]

Kojima K, Brown EC, Rothermel R, Carlson A, Fuerst D, Matsuzaki N, Shah A, Atkinson M, Basha M, Mittal S, et al. Clinical significance and developmental changes of auditory-language-related gamma activity. Clin. Neurophysiol. 2013; 124:857–869. [PubMed: 23141882]

Korovaichuk A, Makarova J, Makarov Va, Benito N, Herreras O. Minor contribution of principal excitatory pathways to hippocampal LFPs in the anesthetized rat: a combined independent component and current source density study. J. Neurophysiol. 2010; 104:484–497. [PubMed: 20463202]

Lee S, Buchsbaum MS. Topographic mapping of EEG artifacts. Clin. EEG Electroencephalogr. 1987; 18:61–67.

Lee T-W, Girolami M, Sejnowski TJ. Independent component analysis using an extended infomax algorithm for mixed subgaussian and supergaussian sources. Neural Comput. 1999; 11:417–441. [PubMed: 9950738]

Liu ZJ, Ikeda K, Harada S, Kasahara Y, Ito G. Functional properties of jaw and tongue muscles in rats fed a liquid diet after being weaned. J. Dent. Res. 1998; 77:366–376. [PubMed: 9465169]

Logothetis NK, Pauls J, Augath M, Trinath T, Oeltermann A. Neurophysiological investigation of the basis of the fMRI signal. Nature. 2001; 412:150–157. [PubMed: 11449264]

Makarov VA, Makarova J, Herreras O. Disentanglement of local field potential sources by independent component analysis. J. Comput. Neurosci. 2010; 29:445–457. [PubMed: 20094907]

Makarova J, Ortuño T, Korovaichuk A, Cudeiro J, Makarov Va, Rivadulla C, Herreras O. Can pathway-specific LFPs be obtained in cytoarchitectonically complex structures? Front. Syst. Neurosci. 2014; 8:66. [PubMed: 24822038]

Makeig S, Jung TP, Bell AJ, Ghahremani D, Sejnowski TJ. Blind separation of auditory event-related brain responses into independent components. Proc. Natl. Acad. Sci. U. S. A. 1997; 94:10979–10984. [PubMed: 9380745]

Markowitz DA, Wong YT, Gray CM, Pesaran B. Optimizing the decoding of movement goals from local field potentials in macaque cortex. J. Neurosci. 2011; 31:18412–18422. [PubMed: 22171043]

Martín-Vázquez G, Makarova J, Makarov VA, Herreras O. Determining the true polarity and amplitude of synaptic currents underlying gamma oscillations of local field potentials. PLoS One. 2013; 8:e75499. [PubMed: 24073269]

Mitzdorf U. Current source-density method and application in cat cerebral cortex: investigation of evoked potentials and EEG phenomena. Physiol. Rev. 1985; 65:37–100. [PubMed: 3880898]

Nagasawa T, Matsuzaki N, Juhász C, Hanazawa A, Shah A, Mittal S, Sood S, Asano E. Occipital gamma-oscillations modulated during eye movement tasks: simultaneous eye tracking and electrocorticography recording in epileptic patients. NeuroImage. 2011; 58:1101–1109. [PubMed: 21816225]

Nelson MJ, Pouget P, Nilsen EA, Patten CD, Schall JD. Review of signal distortion through metal microelectrode recording circuits and filters. J. Neurosci. Methods. 2008; 169:141–157. [PubMed: 18242715]

Nguyen DP, Lin S-C. A frontal cortex event-related potential driven by the basal forebrain. eLife. 2014; 3:e02148. [PubMed: 24714497]

Nicolelis MA, Ghazanfar AA, Faggin BM, Votaw S, Oliveira LM. Reconstructing the engram: simultaneous, multisite, many single neuron recordings. Neuron. 1997; 18:529–537. [PubMed: 9136763]

Novikov E, Novikov A, Shannahoff-Khalsa D, Schwartz B, Wright J. Scale-similar activity in the brain. Phys. Rev. E. 1997; 56:R2387–R2389.

Nunez, PL.; Srinivasan, R. Electric Fields of the Brain: The Neurophysics of EEG. New York, New York: Oxford University Press; 2006.

Nunez DPL, Westdorp AF. The surface laplacian, high resolution EEG and controversies. Brain Topogr. 1994; 6:221–226. [PubMed: 8204409]

Nunez PL, Srinivasan R, Westdorp AF, Wijesinghe RS, Tucker DM, Silberstein RB, Cadusch PJ. EEG coherency I: statistics, reference electrode, volume conduction, Laplacians, cortical imaging, and interpretation at multiple scales. Electroencephalogr. Clin. Neurophysiol. 1997; 103:499–515.

Paxinos, G.; Watson, C. The Rat Brain in Stereotaxic Coordinates. London: Academic Press; 2007.

Pesaran B, Pezaris JS, Sahani M, Mitra PP, Andersen RA. Temporal structure in neuronal activity during working memory in macaque parietal cortex. Nat. Neurosci. 2002; 5:805–811. [PubMed: 12134152]

Raimondo F, Kamienkowski JE, Sigman M, Fernandez Slezak D. CUDAICA: GPU optimization of infomax-ICA EEG analysis. Comput. Intell. Neurosci. 2012:2012.

Ranta, R.; Salido-Ruiz, R.; Louis-Dorr, V. Reference estimation in EEG recordings; 2010 Annual International Conference of the IEEE Engineering in Medicine and Biology Society (EMBC); 2010. p. 5371-5374.

Raver SM, Lin S-C. Basal forebrain motivational salience signal enhances cortical processing and decision speed. Front. Behav. Neurosci. 2015; 9:1–12. [PubMed: 25653603]

Schroeder CE, Tenke CE, Givre SJ, Arezzo JC, Vaughan HG. Striate cortical contribution to the surface-recorded pattern-reversal VEP in the alert monkey. Vis. Res. 1991; 31:1143–1157. [PubMed: 1891808]

Srinivasan R, Nunez PL, Silberstein RB. Spatial filtering and neocortical dynamics: estimates of EEG coherence. IEEE Trans. Biomed. Eng. 1998; 45:814–826. [PubMed: 9644890]

Steinschneider M, Tenke CE, Schroeder CE, Javitt DC, Simpson GV, Arezzo JC, Vaughan HG. Cellular generators of the cortical auditory evoked potential initial component. Electroencephalogr. Clin. Neurophysiol. 1992; 84:196–200.

Uchida K, Yamada Y, Sato T. The coordination of rhythmical drinking behavior with swallowing in rabbits. Physiol. Behav. 1994; 55:795–801. [PubMed: 8022896]

Vetter RJ, Williams JC, Hetke JF, Nunamaker EA, Kipke DR. Chronic neural recording using silicon-substrate microelectrode arrays implanted in cerebral cortex. IEEE Trans. Biomed. Eng. 2004; 51:896–904. [PubMed: 15188856]

Whitham EM, Pope KJ, Fitzgibbon SP, Lewis T, Clark CR, Loveless S, Broberg M, Wallace A, DeLosAngeles D, Lillie P, et al. Scalp electrical recording during paralysis: quantitative evidence that EEG frequencies above 20 Hz are contaminated by EMG. Clin. Neurophysiol. Off. J. Int. Fed. Clin. Neurophysiol. 2007; 118:1877–1888.

Yamamoto T, Matsuo R, Fujiwara T, Kawamura Y. EMG activities of masticatory muscles during licking in rats. Physiol. Behav. 1982; 29:905–913. [PubMed: 7156228]

Yuval-Greenberg S, Tomer O, Keren AS, Nelken I, Deouell LY. Transient induced gamma-band response in EEG as a manifestation of miniature saccades. Neuron. 2008; 58:429–441. [PubMed: 18466752]

Zaveri HP, Duckrow RB, Spencer SS. On the use of bipolar montages for time-series analysis of intracranial electroencephalograms. Clin. Neurophysiol. 2006; 117:2102–2108. [PubMed: 16887380]

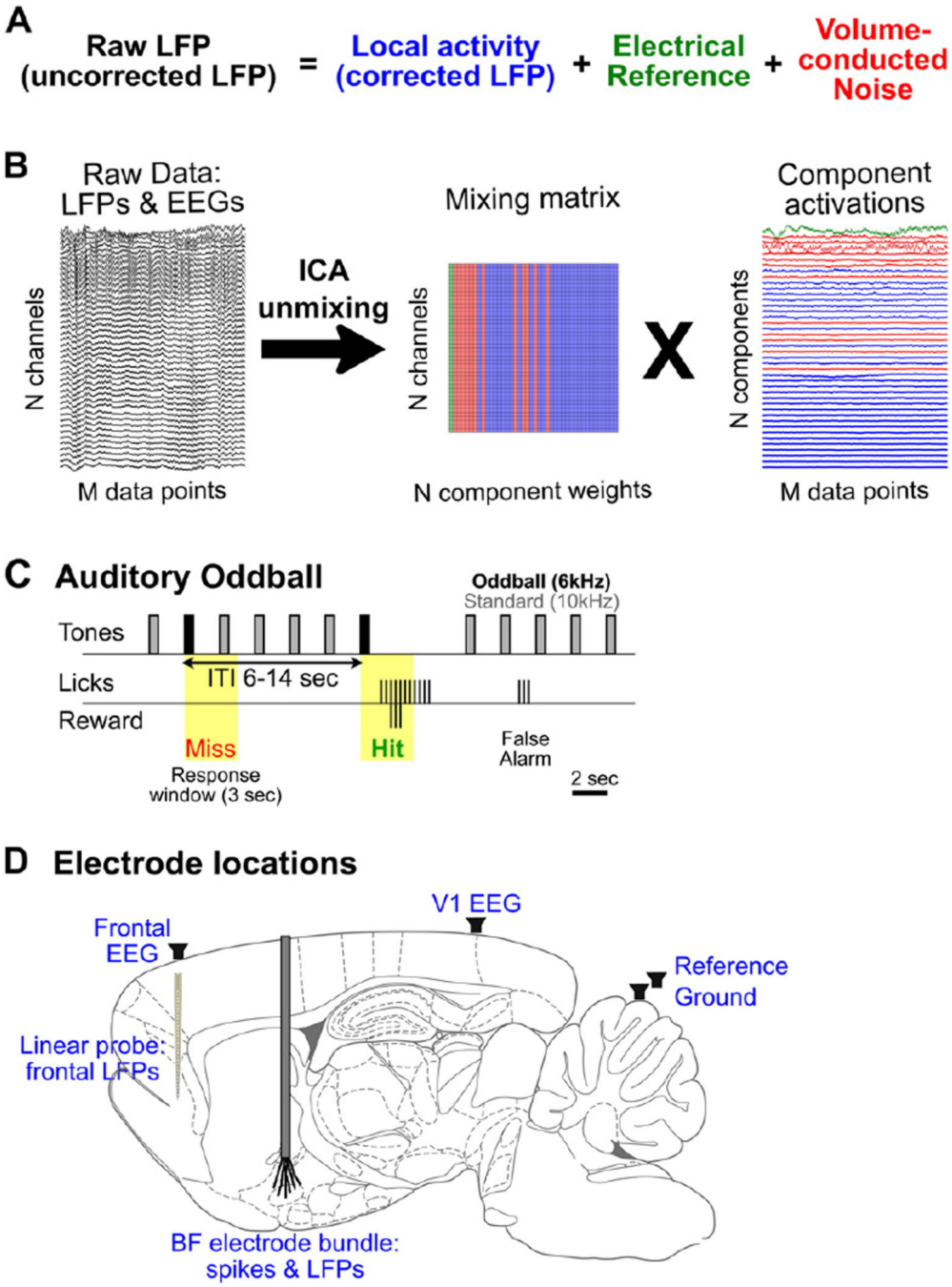

Fig. 1.

Schematic of ICA decomposition and LFP/EEG recording in the auditory oddball task (A) The hypothesis tested in this study specified that LFP signals are consisted of a mix of true local activity (blue) and distal sources, including electrical signals at the reference site (green) and other volume-conducted noise (red). The same color labels are used throughout all figures. (B) Schematic of the ICA analysis. Epochs of LFP and EEG signals around tone onsets were transformed by ICA into the product of a mixing matrix and underlying signal sources called Independent Components (ICs). ICs were classified into the three categories:

electrical reference, volume-conducted noise, and local activity. The mixing matrix describes the weights with which ICs are added together to recreate the original signal in each channel. (C) In the auditory oddball task, a standard tone (10 kHz) was presented once every 2 s, and occasionally once every 6–14 s, a deviant oddball tone (6 kHz) was presented that signaled reward if responded to within a 3-s window (yellow). (D) Schematic of the recording configuration. LFPs were simultaneously recorded from a 32-channel linear probe spanning multiple cortical layers in the frontal cortex, and from multi-electrode bundles in bilateral BF. In addition, EEG signals from the frontal cortex and visual cortex were recorded with skull screws. Electrical reference was a skull screw over the cerebellum.

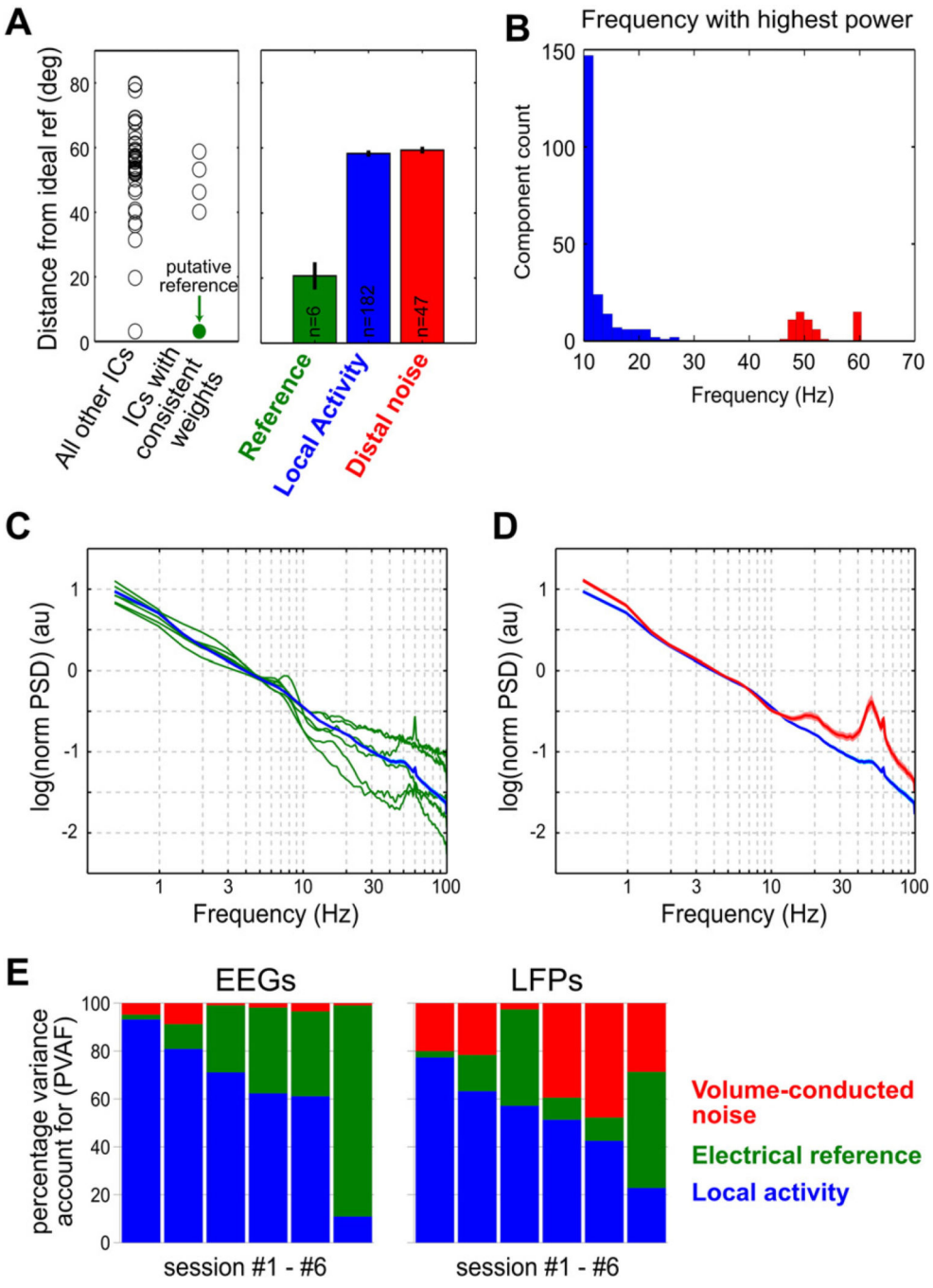

Fig. 2.

Identification of distal electrical signals originating from electrical reference and volume-conducted noise (A) Left, data from one example session illustrate the identification of the reference signal IC. For each IC, the vector angle between its weights across channels and a vector representing an ideal reference signal with equal weights on all channels was calculated. A single IC representing the electrical signal from the reference site was defined as the IC whose weights had a consistent sign across all channels and from this group the IC with the smallest variation in weight across channels (smallest vector angle, solid green

circle). Right, mean distance from the ideal reference for each class of IC across all sessions. (B) Histogram of the peak frequency of non-reference ICs from all sessions reveals a bimodal distribution. ICs with peak frequencies above 45 Hz were identified as volume-conducted noise ICs (red). (C) Log–log plot of the power spectral density of the reference IC from each of the six sessions (green) compared to local ICs (blue, mean ± SEM). The power spectral density of reference ICs deviates from the $1/f$ power-frequency scaling observed in local ICs, particularly at high frequencies. (D) Log–log plot of the power spectral density of volume-conducted noise ICs (red, mean ± SEM) compared to local ICs (blue, mean ± SEM). The power spectral density of noise ICs also deviates from the $1/f$ relationship and show a broad peak at 40–60 Hz as well as a narrow peak at 60 Hz corresponding to line noise. (E) The percentage variance accounted for (PVAF) by local activity, electrical reference and volume-conducted noise in each of the six sessions ($n = 5$ rats), plotted separated for EEG and LFP signals. Sessions were separately sorted for EEGs (left) and LFPs (right) by descending PVAF accounted for by putative local activity ICs.

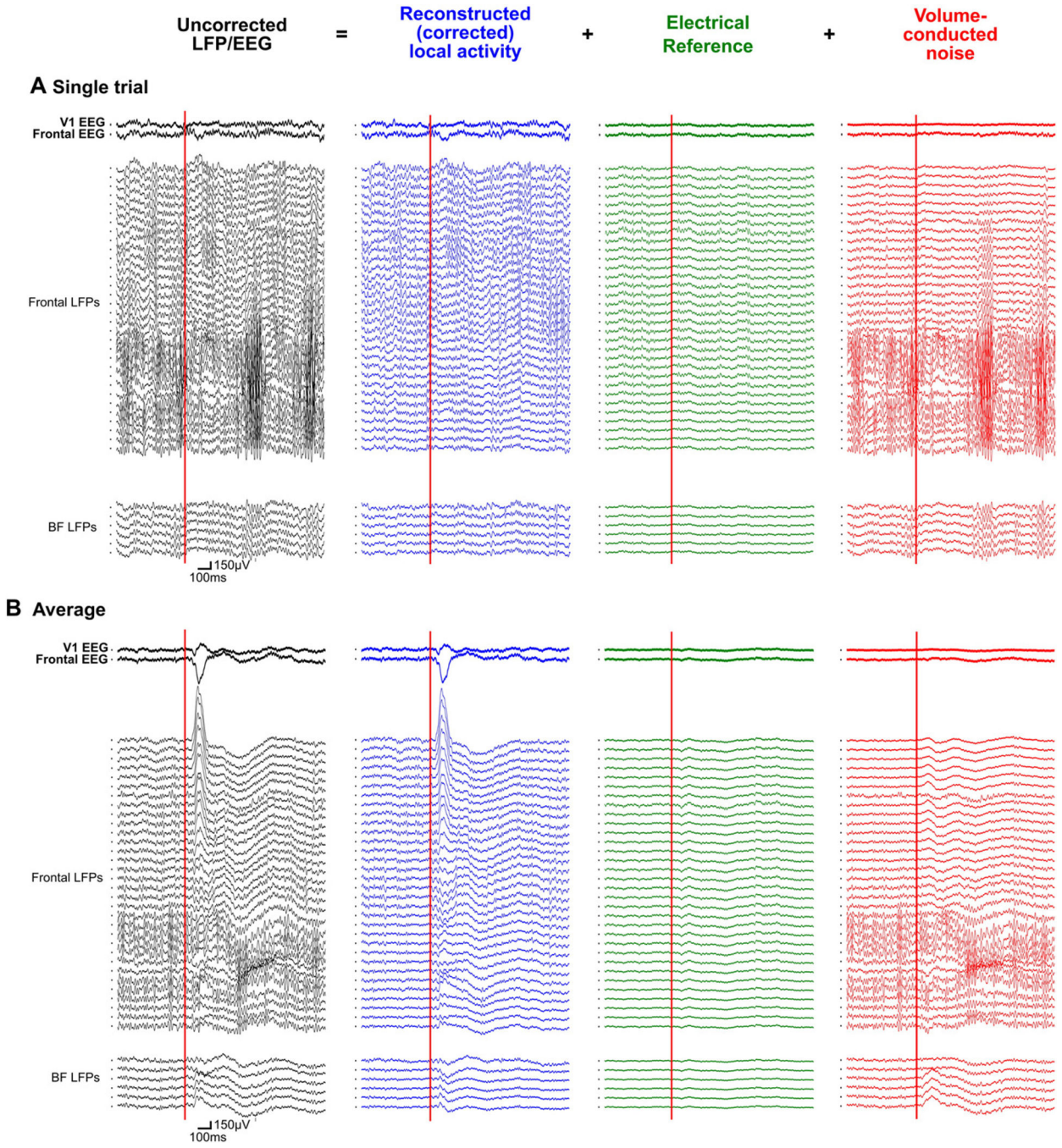

Fig. 3.

An example of how raw LFP/EEG signals are partitioned into three distinct signal sources (A) Activity from a single oddball trial was partitioned into the sum of local activity, electrical reference and volume-conducted noise signals based on ICA transformation. Removal of distal electrical signals unmasked the dynamics of LFP/EEG signals in single trials. Red vertical lines indicate oddball sound onset. (B) Average LFP/EEG signals of all oddball hit trials from the same session. The main features of event-related responses in both EEGs and LFPs were preserved in the local activity, while volume-conducted noise and

electrical reference contributed little to the average response. The mark to the left of each trace indicates zero in the y-axis.

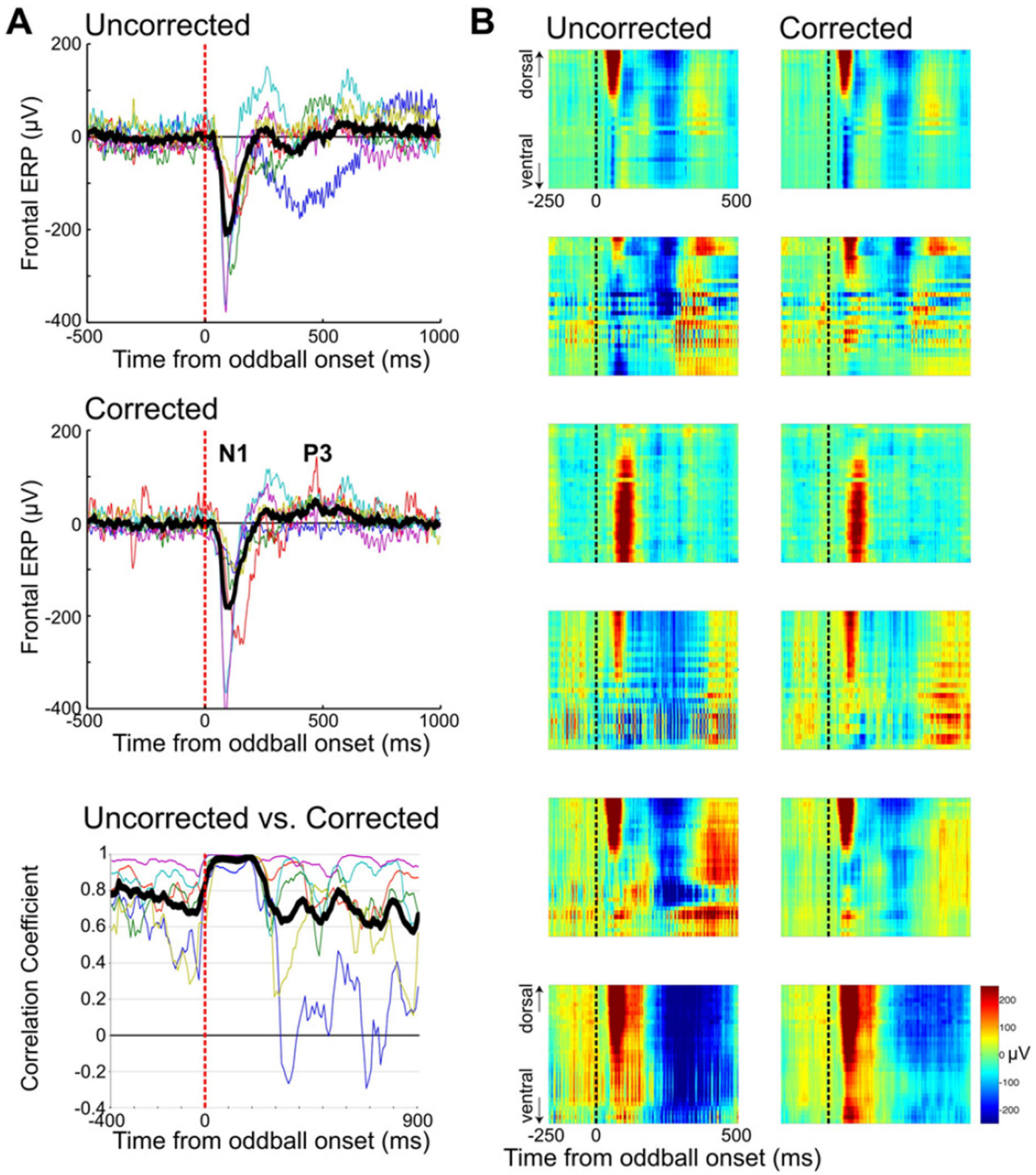

Fig. 4.

ERP and layer-specific LFP responses are preserved in reconstructed local activity (A) Frontal ERPs from all sessions (colored lines) and the group mean (black), before (top) and after (middle) removing volume-conducted noise and reference ICs. Bottom, pre- and post-correction ERPs were highly similar in the N1-like component window, measured by sliding window cross correlation. Also note that the correction procedure made longer latency ERPs more consistent across sessions and revealed a P3-like component. (B) Comparison of layer-specific frontal LFP responses in oddball hit trials before and after the removal of distal

electrical signals in all six sessions. Removing distal electrical signals significantly reduced layer-nonspecific high-frequency noise, while preserving the layer-specific LFP response pattern in the N1-like component window. Sessions were sorted in the same order as the right panel in Fig. 2E. Sessions 1 and 5 were from the same animal.

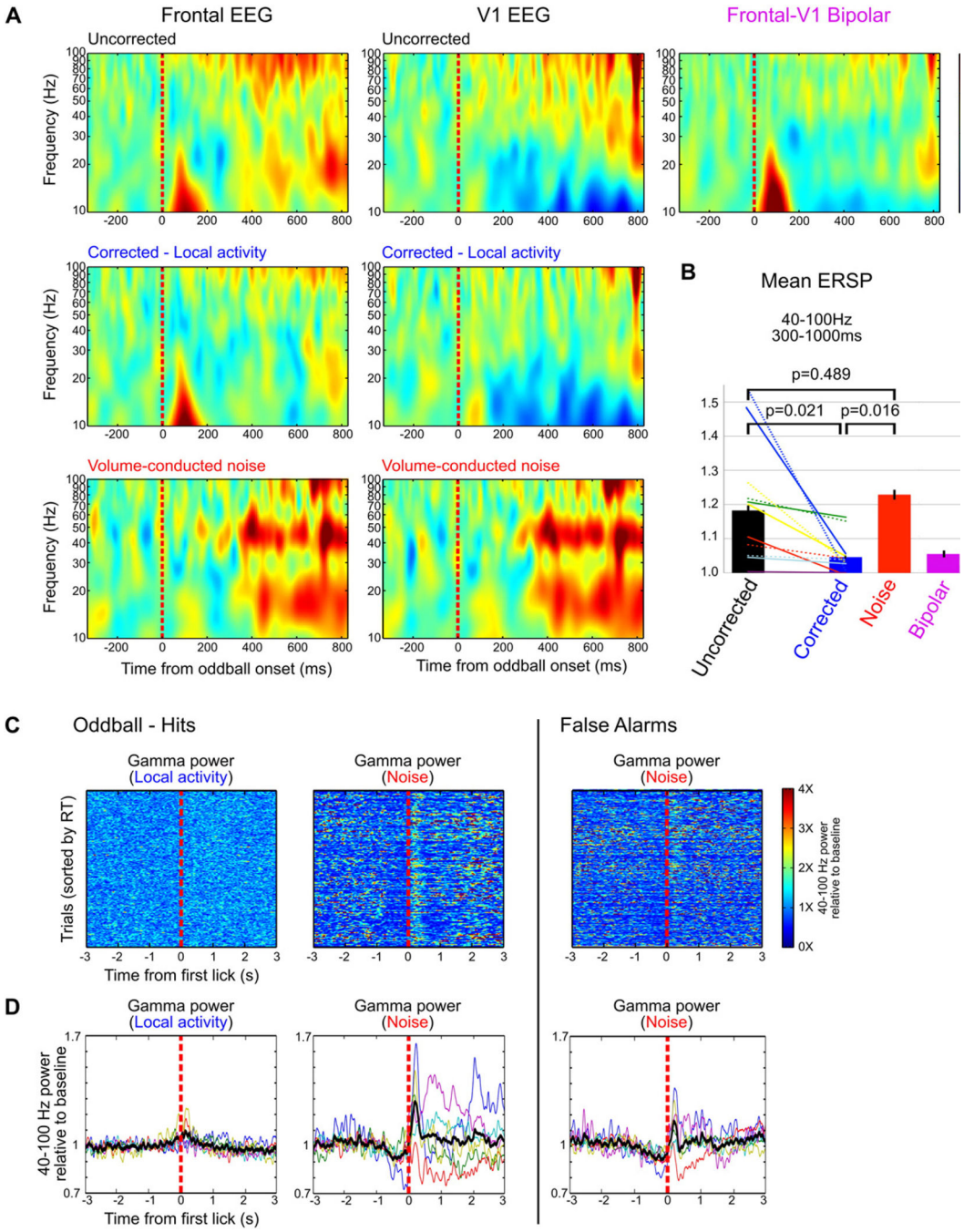

Fig. 5.

Removal of distal electrical signals affects event-related spectral perturbation (A) Event-related spectral perturbation (ERSP) in oddball hit trials, averaged across all six sessions. Increased gamma oscillation (40–100 Hz) power at long latencies (> 300 ms) was prominent in both the frontal (left) and the visual cortex (right) EEGs prior to the removal of distal electrical signals (top) but was reduced after the correction (middle). Strong long-latency gamma ERSP was observed in the volume-conducted noise (bottom) and was largely eliminated in a frontal-V1 bipolar derivation of the uncorrected data (top right), confirming

that the gamma ERSP resulted primarily from signals common to the frontal and V1 EEGs. (B) Mean ERSP in oddball hit trials, averaged across 40–100 Hz between 300 and 1000 ms was significantly reduced after the removal of distal electrical signals ($p = 0.021$, 2-tailed paired *t*-test). Most of the gamma range ERSP in the uncorrected EEGs was instead preserved in the noise components. Data from the frontal (solid line) and the visual cortex (dashed line) were combined. Each session was color coded as in Fig. 4A. (C and D) Single-trial gamma oscillation amplitude in the frontal EEG in a representative session (C) and averaged for each session ($n = 6$) (D), aligned at the first Lick. *gamma* oscillation amplitude in oddball hit trials showed a stereotypical increase in noise components (middle) but not in local components (left), coincident with the start of licking. This pattern of gamma oscillation increase was similarly present when rats licked outside of the reward window (right, false alarms). Each session in (D) was color coded as in Fig. 4A.

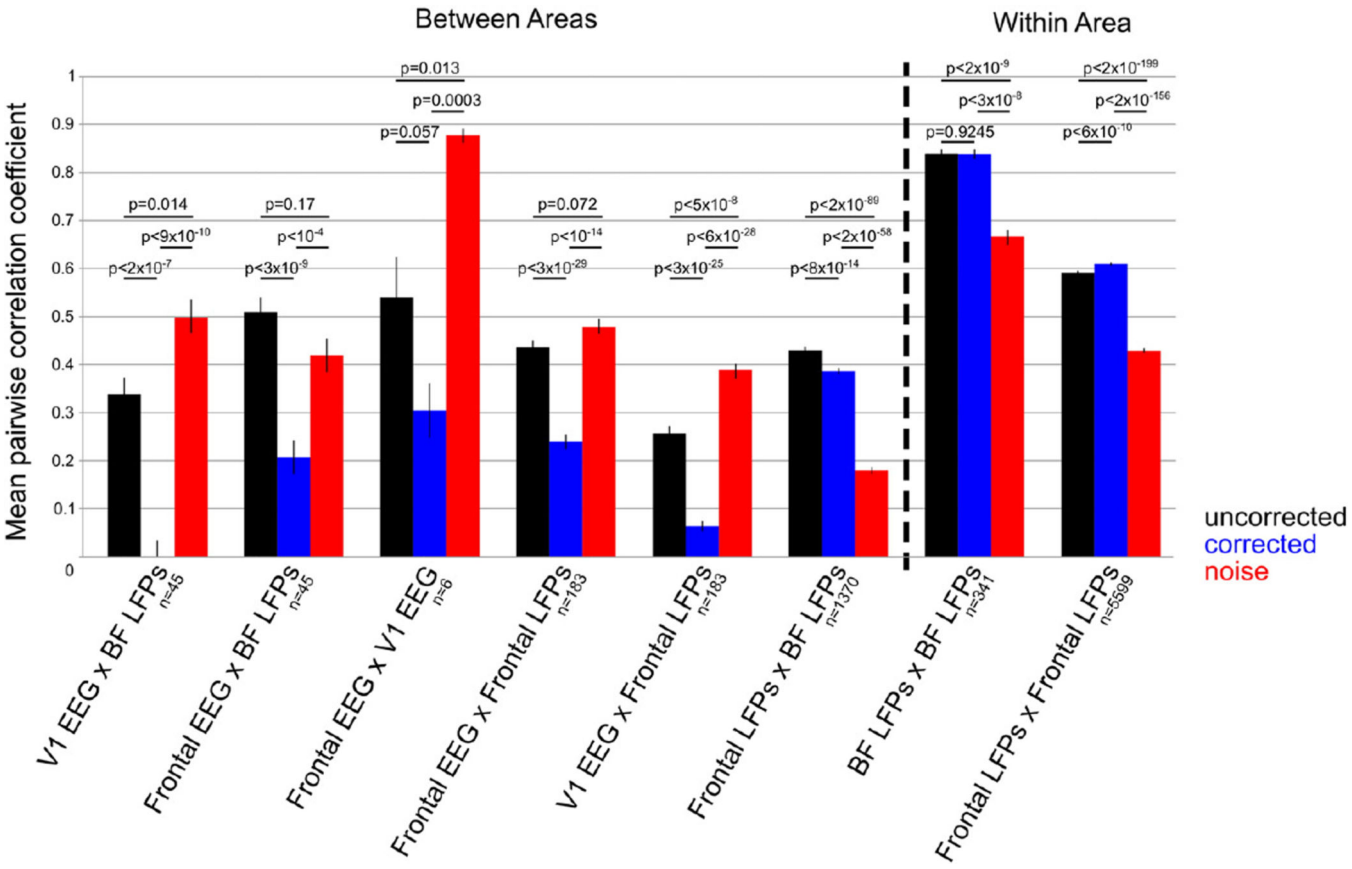

Fig. 6.

Removal of distal electrical signals selectively reduces correlation between distant brain regions Correlation coefficients (mean ± SEM) of un-averaged time series between channel pairs within and between different brain regions, plotted separately for uncorrected (black), corrected (blue), and volume-conducted noise (red) signals. Removal of distal electrical signals significantly decreased the mean correlation of pairs of recordings that spanned two different brain regions but did not decrease correlation between recordings within the same region (2 tailed paired *t*-test). On the other hand, the aggregate volume-conducted noise was highly correlated across distant brain regions compared to local activity.

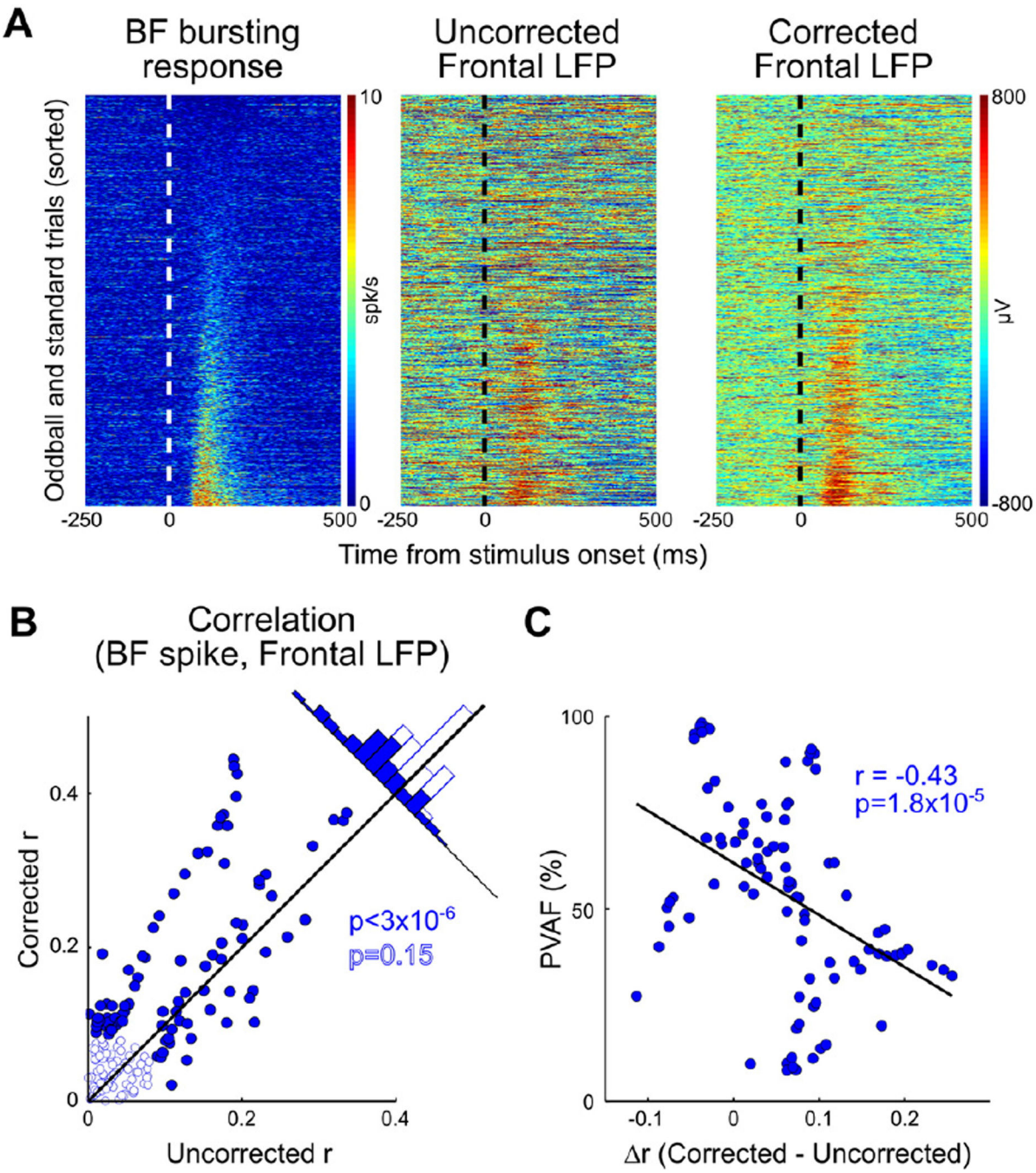

Fig. 7.

Removal of distal electrical signals improves single-trial amplitude coupling between frontal LFP and BF neuronal activity (A) An example session showing single-trial BF bursting activity (left) and one representative frontal LFP channel, before (middle) and after (right) the removal of distal electrical signals. Oddball and standard trials were pooled and sorted based on BF bursting amplitude in the 50- to 200-ms window. The single-trial coupling between BF bursting amplitude and frontal LFP activity was significantly enhanced after the correction. (B) Scatter plot showing correlation coefficients between single-trial BF bursting

strength and frontal LFP amplitude, before (abscissa) and after (ordinate) the removal of distal electrical signals. Each dot represents one frontal LFP channel in one session. LFP channels showing a significant correlation with BF bursting strength ($p < 0.0001$) are indicated by filled symbols. Histogram along the diagonal line shows a significant increase in correlation coefficients after the removal of distal electrical signals for significantly correlated frontal LFP channels ($p < 3 \times 10^{-6}$) but not for uncorrelated frontal LFP channels ($p = 0.15$, 2-tailed paired *t*-test). (C) In frontal LFP channels that were significantly correlated with BF bursting strength, the change in correlation coefficients induced by the removal of distal electrical signals was negatively correlated with the amount of variance explained by local activity in the uncorrected LFP in each channel.